Cellular and Molecular Life Sciences (2018) 75:2257–2271
https://doi.org/10.1007/s00018-017-2732-5

ORIGINAL ARTICLE

Delta opioid receptors recycle to the membrane after sorting to the degradation path

Iness Charfi[1,4] · Khaled Abdallah[2] · Louis Gendron[2] · Graciela Pineyro[1,3,4]

Received: 8 June 2017 / Revised: 29 November 2017 / Accepted: 18 December 2017 / Published online: 29 December 2017

Abstract

Soon after internalization delta opioid receptors (DOPrs) are committed to the degradation path by G protein-coupled receptor (GPCR)-associated binding protein. Here we provide evidence that this classical post-endocytic itinerary may be rectified by downstream sorting decisions which allow DOPrs to regain to the membrane after having reached late endosomes (LE). The LE sorting mechanism involved ESCRT accessory protein Alix and the TIP47/Rab9 retrieval complex which supported translocation of the receptor to the TGN, from where it subsequently regained the cell membrane. Preventing DOPrs from completing this itinerary precipitated acute analgesic tolerance to the agonist DPDPE, supporting the relevance of this recycling path in maintaining the analgesic response by this receptor. Taken together, these findings reveal a post-endocytic itinerary where GPCRs that have been sorted for degradation can still recycle to the membrane.

Keywords Delta opioid receptor · Recycling · Analgesic tolerance · Trans-Golgi network · Rab9/TIP47 complex · Alix

Introduction

Displaying both higher efficacy for chronic pain management and a better side effects profile than analgesics activating mu opioid receptors (MORs), delta opioid receptor (DOPr) ligands have emerged as an attractive alternative for pain treatment [1, 2]. On the other hand, analgesic tolerance remains a real concern associated with DOPr agonists, justifying considerable efforts to understand how this side effect develops [3–5]. Efficacy to induce DOPr sequestration has been proposed as a predictor of agonist tendency to induce in vivo analgesic tolerance [2, 5]. This hypothesis is supported by observations indicating that internalized DOPrs are rapidly committed to the degradation path both in immortalized cell lines [6, 7] and in native neurons [8]. At the same time, and despite consistent reports of DOPrs being sorted for degradation [8], these receptors are also known to regain the membrane [9], resensitize [10], and agonists that support recycling produce minimal tolerance [3].

Sorting of cargo to the degradation path relies upon the endosomal sorting complex required for transport (ESCRT). The complex recognizes ubiquitinated receptors on the limiting membrane of early endosomes (EE) and transfers them into intraluminal vesicles (ILVs) of budding multivesicular bodies (MVBs). From there degradative cargo progresses to late endosomes (LEs) and lysosomes (LYS) [11]. Traditionally, ubiquitination was considered the single sorting signal capable of excluding receptors from bulk recycling and committing them to this degradation path [12]. More recently additional sorting machineries have emerged which either direct ubiquitinated GPCRs back to the surface [13] or that support lysosomal targeting of non-ubiquitinated receptors [14, 15]. One of such sorting devices is the GPCR-associated binding protein-1 (GASP1) [7]. This cytoplasmic protein binds to the carboxy-tail of DOPrs [7], dopamine D2 receptors [16] and cannabinoid CB1 receptors [17] excluding them from recycling even before the ESCRT machinery comes into play [6, 18].

Electronic supplementary material The online version of this article (https://doi.org/10.1007/s00018-017-2732-5) contains supplementary material, which is available to authorized users.

✉ Graciela Pineyro
graciela.pineyro.filpo@umontreal.ca

1 Department of Pharmacology, University of Montreal, Montreal, Quebec H3T 1J4, Canada

2 Department of Pharmacology-physiology, University of Sherbrooke, Sherbrooke, Quebec J1H 5N4, Canada

3 Department of Psychiatry, University of Montreal, Montreal, Quebec H3T 1J4, Canada

4 Ste-Justine Hospital, Montreal, Quebec H3T 1C5, Canada

In the present study we were interested in finding out how internalized DOPrs that are subject to GASP-1 action [7, 18] can still recycle to the membrane. Results obtained showed that neither Rab4-dependent carriers nor the retromer contributed to DOPr recycling in neurons or immortalized cell-lines. Instead, recycling DOPrs relied on the ALG-2-interacting Protein X (ALIX) and the Rab9/TIP47 retrieval complex, to regain the membrane from LEs via the trans-golgi-network (TGN). Furthermore, agents that prevented DOPrs from completing this itinerary also precipitated analgesic tolerance, indicating that a recycling path originating from degradation-related compartments contributes to maintaining the in vivo analgesic response to DOPr activation.

Results

DOPr recycling to the membrane is blocked by interfering with Rab7 but not retromer action

It is well documented that DOPrs are sorted to the LYS upon internalization [7], but they are also known to recycle back to the surface [3, 9]. Here we were interested in establishing the mechanism that supports membrane recovery of internalized DOPrs. To address this question we monitored DOPr trafficking in cortical neuron cultures. Thus, in the first series of measures, Flag-DOPrs were labeled with primary antibody at the neuron's surface, cultures were exposed to DPDPE (10 μM, 60 min) or vehicle (0.05% DMSO) and at end of treatment cultures were washed to remove drugs as well as antibody that remained bound to non-internalized receptors. After wash, a set of these neurons was immediately processed to specifically reveal intracellular immunoreactivity corresponding either to constitutive (vehicle) or DPDPE-induced internalization of surface-labeled DOPrs (Fig. 1a). Another group of neurons was allowed to recover 60 min in the absence of ligand (Fig. 1a) before revealing intracellular immunoreactivity. In-keeping with previous observations [3], mean intracellular labeling density was less in cultures that were allowed to recover from DPDPE treatment than in neurons that were fixed immediately after treatment (41.88 ± 2.6% reduction; $p < 0.0001$; $n = 18$; Fig. 1b), indicating that receptors that had been internalized by DPDPE left the intracellular compartment upon removal of the agonist. In parallel, and so as to confirm that at least part of the receptors leaving the cytoplasm relocated to the membrane, immunoreactivity of recovered cells was assessed in non-permeabilized neurons so as to specifically reveal DOPrs that had regained the surface (Fig. 1a). Consistent with recycling, surface labeling was present in neurons in which Flag-DOPrs had been internalized by the agonist but practically absent in neurons where receptors had been constitutively internalized (Fig. 1c). These changes in intracellular and surface labeling density were subsequently monitored so as to trace a "functional itinerary" for recycling DOPrs.

Recycling cargo may first exit the endosomal compartment from a network of tubules where structures decorated with Rab4 and Rab5 or Rab4 and Rab11, respectively, support fast and slow recycling [19]. The possibility that DOPr recycling involved these structures was ruled by the observation that recovery from DPDPE treatment caused similar changes in intracellular and surface labeling in neurons transfected with a dominant-negative mutant of Rab4 (Rab4N121I) [20] and its empty vector (Supplementary figure 1a and Supplementary Table 1). This same mutant was also without effect in HEK cells, where similar proportion of internalized receptors recycled to the membrane whether Rab4N121I was transfected or not (Supplementary figure 1b).

Cargo that is not recycled through the tubular network is progressively sorted to degradation [21], a mechanism which effectively operates on DOPrs [18]. However, DOPrs could be rescued back to the membrane before entering the degradation path through coordinated action of Rab7 [22] and the retromer [23], which together retrieve cargo from the endosomal compartment to the TGN. Hence, to determine whether recycling DOPrs left the endosomal compartment at this sorting station, we assessed consequences of interfering either with Rab7 or retromer function. We first observed that in neurons transfected with the inactive Rab7 mutant (Rab7N125I), DOPrs internalized by DPDPE remained trapped within the cytoplasm during recovery from treatment, as indicated by similar intracellular labeling density in agonist-treated neurons which were allowed to recover from agonist exposure (45.3 ± 2.6 arbitrary units) and those that were fixed immediately after internalization (47.8 ± 2.5 arbitrary units; $p > 0.05$; $n = 18$; Fig. 2a). Moreover, neurons expressing inactive Rab7 also failed to display increase in Flag-DOPr surface labeling (Fig. 2a and Supplementary Table 1), confirming that interfering with Rab7 function prevented internalized DOPrs from recycling to the surface.

Rab7 contributes to recruit the retromer's cargo selective complex (VPS26/VPS29/VPS35) to the endosomal membrane. Hence to establish the specific contribution of the retromer to DOPr recycling, VPS35 was silenced. Interestingly, and despite visible depletion of VPS35 by siRNA, DOPr recycling was not affected, as indicated by two complementary observations: (1) the proportion of intracellular labeling lost during recovery from DPDPE exposure was similar in neurons transfected with scrambled- and VPS35-siRNA (% reduction of intracellular fluorescence: 48.28 ± 5.4% in scrambled-siRNA; 58.31 ± 4.4% in VPS35 siRNA, $n = 18$, $p = 0.16$; Fig. 2b, and (2) independent of VPS35 silencing DOPr labeling reappeared at the membrane upon removal of the agonist

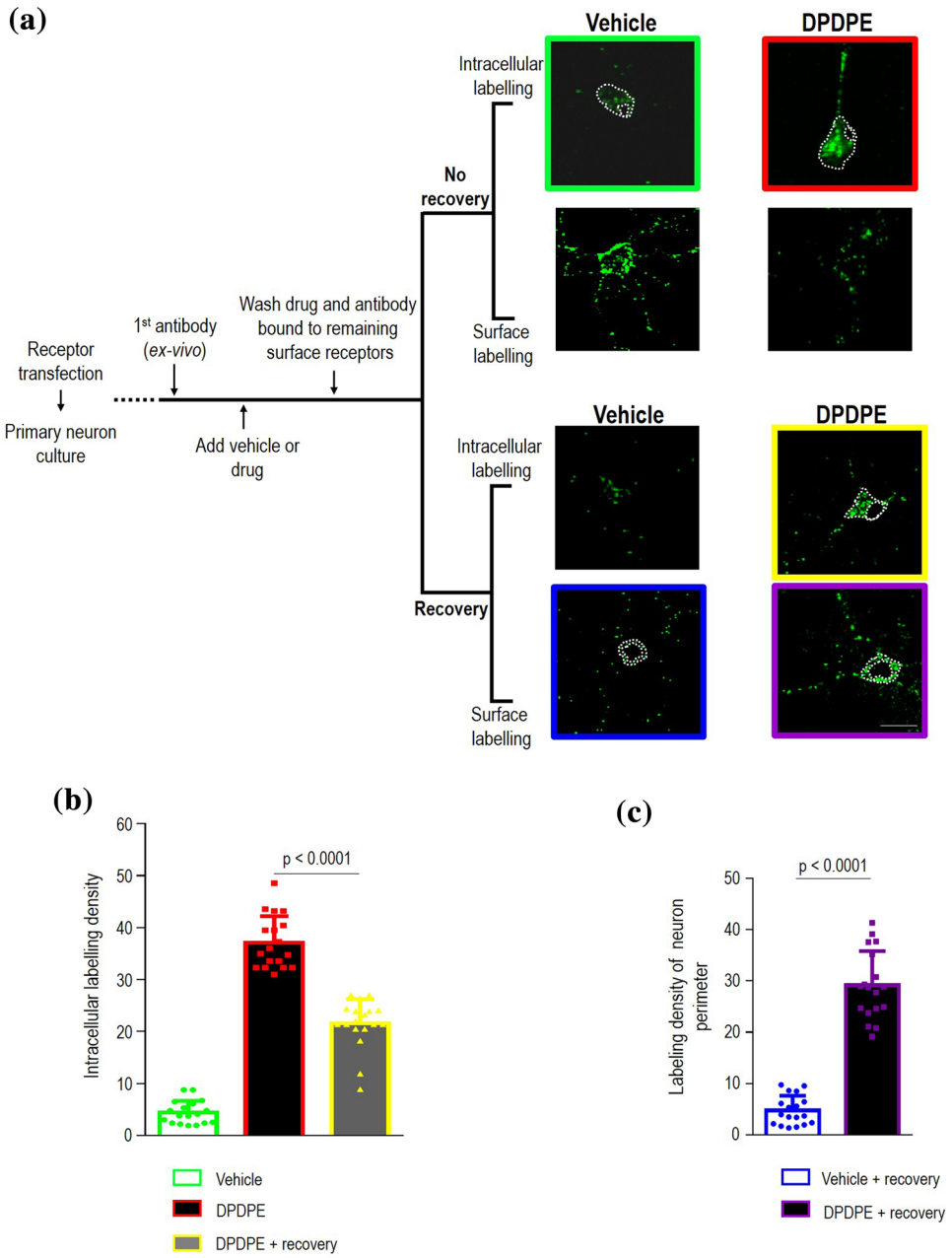

Fig. 1 Quantification of DOPr recycling in neurons. Cortical neurons transfected with Flag-DOPrs were incubated with primary antibody prior to exposure to either vehicle (0.05% DMSO) or DPDPE (10 µM, 60 min). By the end of treatment drug or vehicle were washed-out and antibody bound to remaining surface receptors stripped. At this time one set of cultured neurons was immediately processed for intracellular or surface labeling (no recovery) to, respectively, reveal internalized receptors appearing in the intracellular compartment or disappearing from the surface. Another set of neurons similarly exposed to drug/vehicle were allowed to recover 60 min in the absence of ligand (recovery) before exclusively revealing internalized receptors that remained trapped in the cytoplasm during recovery from treatment or receptors that regained the surface. Dotted white lines delimit regions of interest that were quantified. Scale bar, 50 µm (**a**). Histograms show intracellular labeling density ± SEM (arbitrary units) in neurons labeled immediately after treatment, or neurons that were allowed to recover ($n = 18$ neurons cultured from pups in three different litters). Corresponding scatter plots in red show sample dispersion. Statistical significance was established by one-way ANOVA followed by Tukey's post hoc test which revealed that intracellular labeling following internalization and recovery were different among themselves and from labeling in vehicle-exposed neurons ($p < 0.0001$) (**b**). Histograms and corresponding scatter plots show surface labeling density following 60 min recovery from exposure to DPDPE or vehicle (arbitrary units, $n = 18$). Statistical comparison using non-paired, Student's t test (**c**)

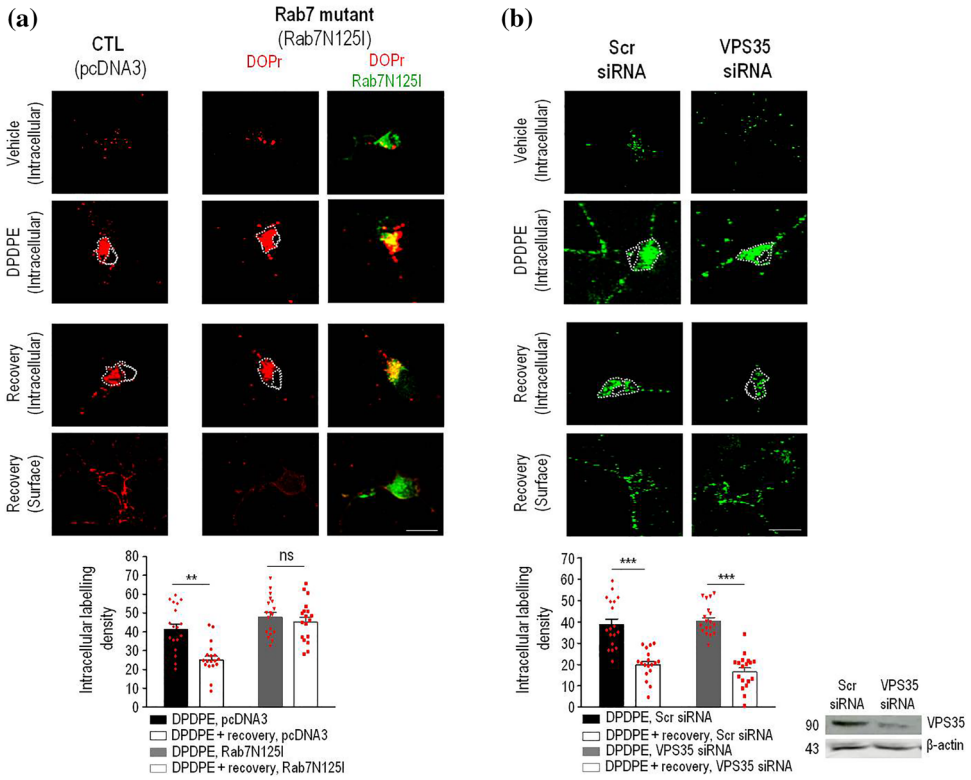

Fig. 2 DOPr recycling is independent of the retromer's cargo-selective complex but blocked by inactive Rab7. Cortical neurons were transfected with Flag-DOPrs (red) and pcDNA3 or Rab7N125I (green) as indicated, treated and processed as in Fig. 1. Upper panels show images illustrating intracellular labeling immediately after end of indicated treatment, lower panels show intracellular and surface labeling in DPDPE-treated cells that were allowed to recover (60 min) in the absence of agonist. Scatter plots and histograms (mean ± SEM; $n = 18$) correspond to intracellular labeling density in neurons processed immediately after DPDPE treatment, and neurons that were allowed to recover from DPDPE exposure as indicated. Comparisons by two-way ANOVA followed by Tukey's post hoc test revealed significant reduction of intracellular labeling following recovery in neurons transfected with pcDNA3 (**$p < 0.001$) but not in Rab7N125I-transfected cells. Scale bar, 50 µm (**a**). Cortical neuron cultures transfected with Flag-DOPrs and either scrambled (Scr-) or VPS35 siRNA were labeled, treated and processed as above to produce scatter plots and histograms (mean ± SEM; $n = 18$) corresponding to intracellular and surface labeling density. Comparisons by two-way ANOVA followed by Tukey's post hoc test revealed significant reduction of intracellular labeling following recovery in scrambled and VPS35 siRNA conditions (***$p < 0.0001$; $n = 18$) (**b**)

(Fig. 2b and Supplementary Table 1). This lack of effect of VPS35 silencing on membrane recovery of DOPrs was in stark contrast with the inhibition of β2ARs recycling (Supplementary figure 2a and 2b, Supplementary Table 1), which are known to regain the membrane through a mechanism requiring the retromer's cargo-selective complex [24]. Moreover, transfecting mutant Rab7N125I or silencing expression of VPS35 in HEK cells had similar effects on DOPr recycling as observed in neurons, the Rab7 mutant reducing membrane recovery of internalized receptors by ~ 49% (Supplementary figure 2c), and VPS35 silencing producing no effect (Supplementary figure 2d). Thus, observations obtained in two different cell types indicated that DOPr recycling required Rab7, but not the retromer.

DOPr recycling to the membrane requires the LE to TGN retrieval complex Rab9/TIP47

Because inactive Rab7 mutants block cargo progression from EEs to LEs [25, 26], inhibition of DOPr recycling by Rab7N125I implies that receptors must progress to LE to regain the membrane. To corroborate this notion, we determined whether retrieval mechanisms which normally rescue LE cargo from lysosomal degradation could possibly contribute to surface recovery of internalized DOPrs. One of such mechanisms involves the Rab9–TIP47 complex which retrieves mannose-6-phosphate receptors (M6PRs) in LEs to the TGN [27, 28]. Therefore, we started by assessing how individual silencing of each component influenced DOPr recycling. We observed that the proportion of intracellular immunoreactivity that disappeared from the neuron cytoplasm during recovery from DPDPE treatment dropped from 40 ± 5% in scrambled-transfected controls, to 25.5 ± 4% in

cultures transfected with Rab9–siRNA ($n = 18$, $p = 0.0364$; Fig. 3a), while recovery of membrane labeling was concomitantly reduced by Rab9 silencing (Fig. 3a, Supplementary Table 1). Silencing of TIP47, the cytoplasmic effector of Rab9 [27], similarly reduced DOPr recycling in neurons (Fig. 3a, Supplementary Table 1), and silencing of both partners also interfered with membrane recovery of internalized DOPr in HEK cells (Fig. 4a, b), pointing to the Rab9–TIP47 complex as a conserved player in DOPr recycling.

DOPrs that arrive to LEs are located for the most part in ILVs [6, 18]. Their location in the LE lumen brings up the question how do DOPrs become available at the limiting membrane for recovery by the cytoplasmic Rab9–TIP47 complex. It is well documented that ILVs and the limiting endosomal membrane normally undergo iterative cycles of fission and back-fusion [29] regulated by lyso-bis-phosphatidic acid (LBPA) and the ESCRT accessory protein ALIX [30]. Hence, it stands to reason that DOPrs in ILVs may

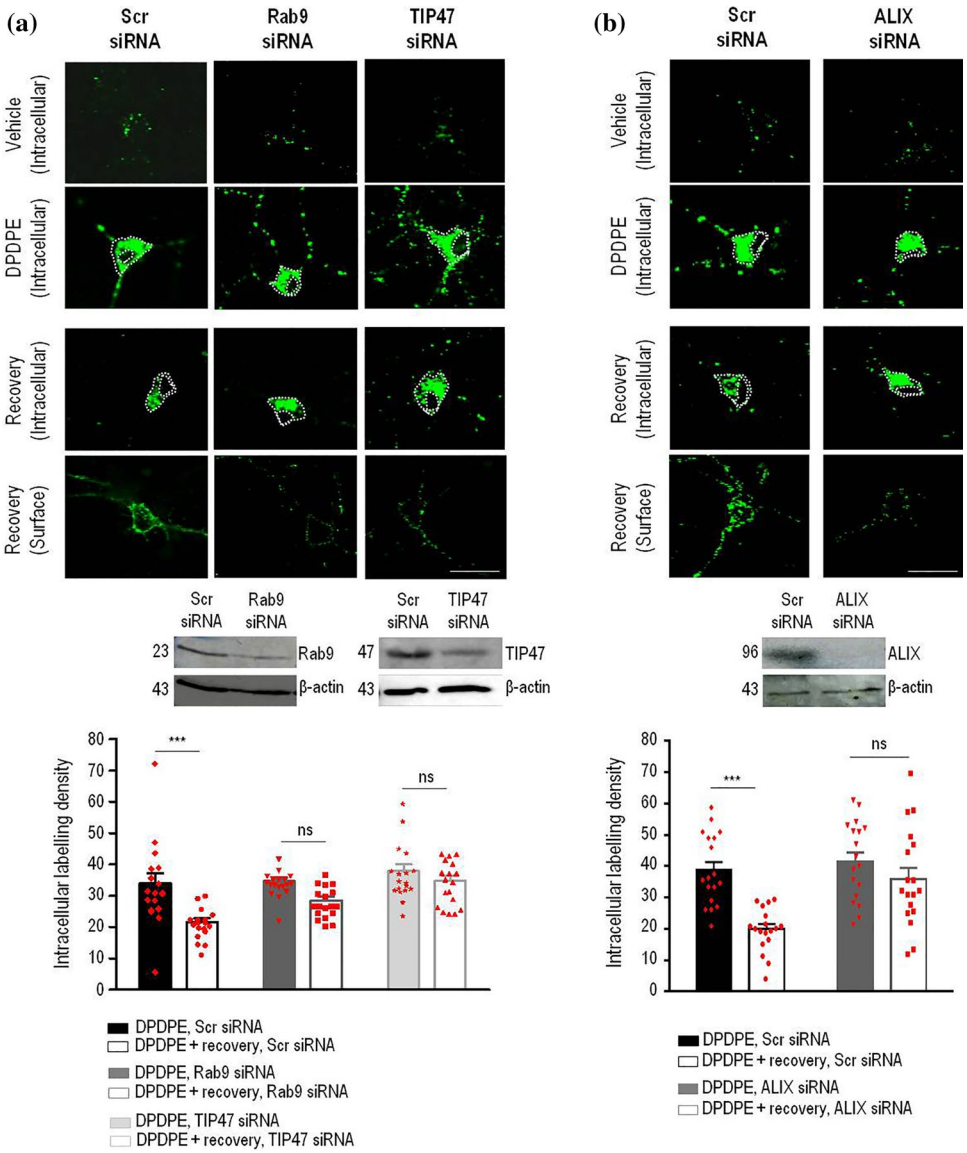

Fig. 3 The Rab9/TIP47 retrieval complex and ESCRT accessory protein ALIX allow DOPrs to recycle back to the membrane in neurons. Cortical neuron cultures transfected with Flag-DOPrs, scrambled-, Rab9 or TIP47 siRNA were labeled and treated as described in Fig. 1. Scatter plots and histograms (mean ± SEM, $n = 18$) show intracellular labeling density obtained immediately after DPDPE treatment or following recovery from agonist exposure. Comparisons by two-way ANOVA followed by Tukey's post hoc test revealed that following recovery from DPDPE treatment intracellular labeling was reduced in neurons transfected with scrambled (***$p < 0.0001$), but not with Rab9 siRNA ($p = 0.0952$), nor TIP47 siRNA ($p = 0.7349$) (**a**). Cortical neuron cultures transfected with Flag-DOPrs and either scrambled (Scr-) or ALIX siRNA, were labeled, treated and processed as above to produce scatter plots and histograms (mean ± SEM; $n = 18$) corresponding to intracellular labeling density. Comparisons by two-way ANOVA followed by Tukey's post hoc test revealed significant reduction of intracellular labeling following recovery in scrambled (***$p < 0.0001$) but not ALIX siRNA-transfected cultures ($p = 0.4793$) (**b**)

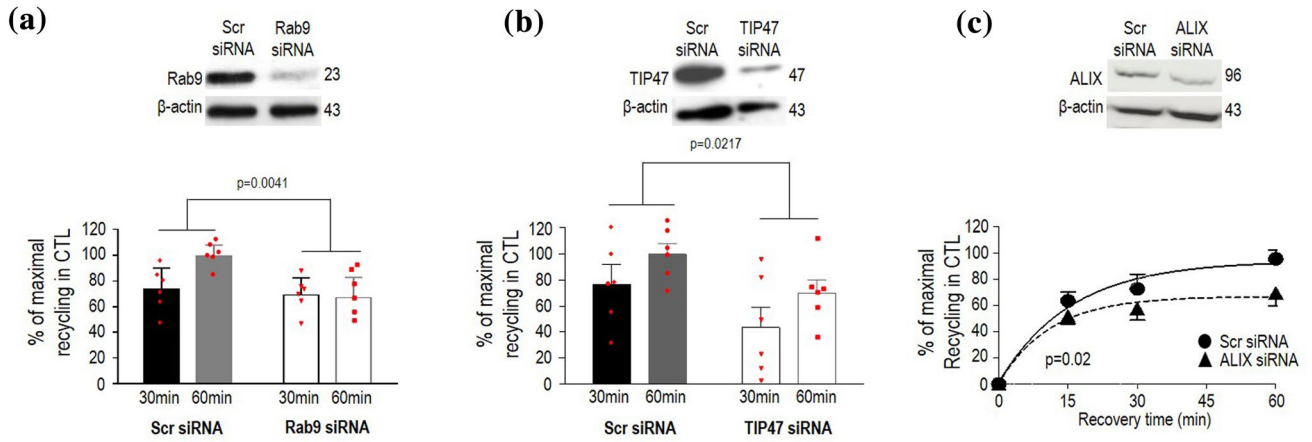

Fig. 4 DOPr recycling by Rab9/TIP47 and ALIX is conserved in HEK293 cells. HEK293 cells expressing Flag-DOPr were transfected with scrambled-, Rab9- (**a**) or TIP47-siRNA (**b**), and recycling evaluated following 30 and 60 min recovery from DPDPE treatment. Results were expressed as % of maximal recycling observed in scrambled-transfected controls, and correspond to mean ± SEM ($n = 6$). Two-way ANOVA followed by Tukey's comparisons revealed an effect of Rab9 siRNA ($p = 0.0041$) and an effect of TIP47 siRNA ($p = 0.0217$). HEK293 cells expressing Flag-DOPr were transfected with scrambled or ALIX siRNA and recycling was evaluated. Results were expressed as % of maximal recycling observed in scrambled-transfected controls and correspond to mean ± SEM ($n = 4$). Curves were fit to one phase exponential kinetics and plateaux for scrambled and ALIX siRNA conditions were compared using 'extra sum of squares F test' revealing a significant difference: plateau scrambled = 94.08 ± 9.12, plateau ALIX siRNA = 66.97 ± 6.87, $p = 0.0462$) (**c**)

rely on back-fusion for their recycling to the membrane. To verify this possibility, we assessed whether DOPr recycling was modified by interfering with ALIX's expression. Consistent with our reasoning, silencing ALIX left intracellular Flag-DOPr immunoreactivity trapped within the neuron cytoplasm (Fig. 3b) prevented the receptor from reappearing at the neuron's surface after recovery from DPDPE treatment (Supplementary Table 1) and also reduced maximal DOPr recycling in HEK cells (Fig. 4c).

Recycling DOPrs reach the membrane from the TGN

Having established that DOPr recycling relies on a mechanism which normally retrieves non-signaling cargo from LEs to the TGN, we then sought to determine whether recycling DOPrs reached the membrane from this compartment. First, we used confocal microscopy to assess the distribution of internalized DOPrs in relation to a resident TGN protein, TGN46. We observed that immediately after DPDPE treatment was finished, DOPrs in the neuron soma colocalized with TGN46 (Supplementary figure 3a).

TGN cargo traffics to the surface through carriers that bud from trans-golgi cisternae and are guided to the membrane by means of the cytoskeleton [31]. Since TGN budding and carrier fission are temperature-sensitive [32], we first assessed if allowing rat cortical neurons to recover from DPDPE exposure at 20 °C rather than 37 °C would influence DOPr recycling. Reducing temperature to 20 °C during recovery from DPDPE treatment caused internalized Flag-DOPrs to remain trapped within the cytoplasm while the amount of labeling reappearing at the membrane was reduced (Fig. 5a, Supplementary Table 1). This was not the case for internalized MOPrs (Supplementary figure 4a, Supplementary Table 1), which unlike DOPrs reach the surface from superficial compartments [33].

From a biochemical standpoint, carrier formation at the TGN relies upon ADP ribosylation factor 1 (ARF1) [31], which in neurons recruits and activates effectors such as actin polymerization factors [34]. In keeping with this mechanism and further supporting the idea that recycling DOPrs regain the membrane from the TGN, transfection with an inactive ARF1-T31N mutant (Fig. 5b) or treatment with actin polymerization blocker cytochalasin D (10 µM; Fig. 6a) [35] prevented internalized DOPrs from leaving the neuron cytoplasm and regaining the surface (Figs. 5b, 6a and Supplementary Table 1) during recovery from DPDPE treatment. It has also been documented that actin-dependent fission of TGN carriers in neurons requires LIMK1 activity [36] and that in the TGN this kinase is activated via Rho-associated coiled-coil containing protein kinase-II (ROCK-II) [37]. When introduced during recovery from DPDPE treatment ROCK inhibitor Y27632 [38] (10 µM) caused internalized receptors to remain trapped within the neuron soma (Fig. 6b) and accumulate with TGN46 (Supplementary figure 3b). Admittedly, decrease in temperature, ARF1 inactivation and interfering with actin polymerization may each affect other pathways in addition to TGN to membrane transport, but their shared ability to interfere with surface recovery of DOPrs allows to conclude that these receptors take the TGN export route on their way to the membrane.

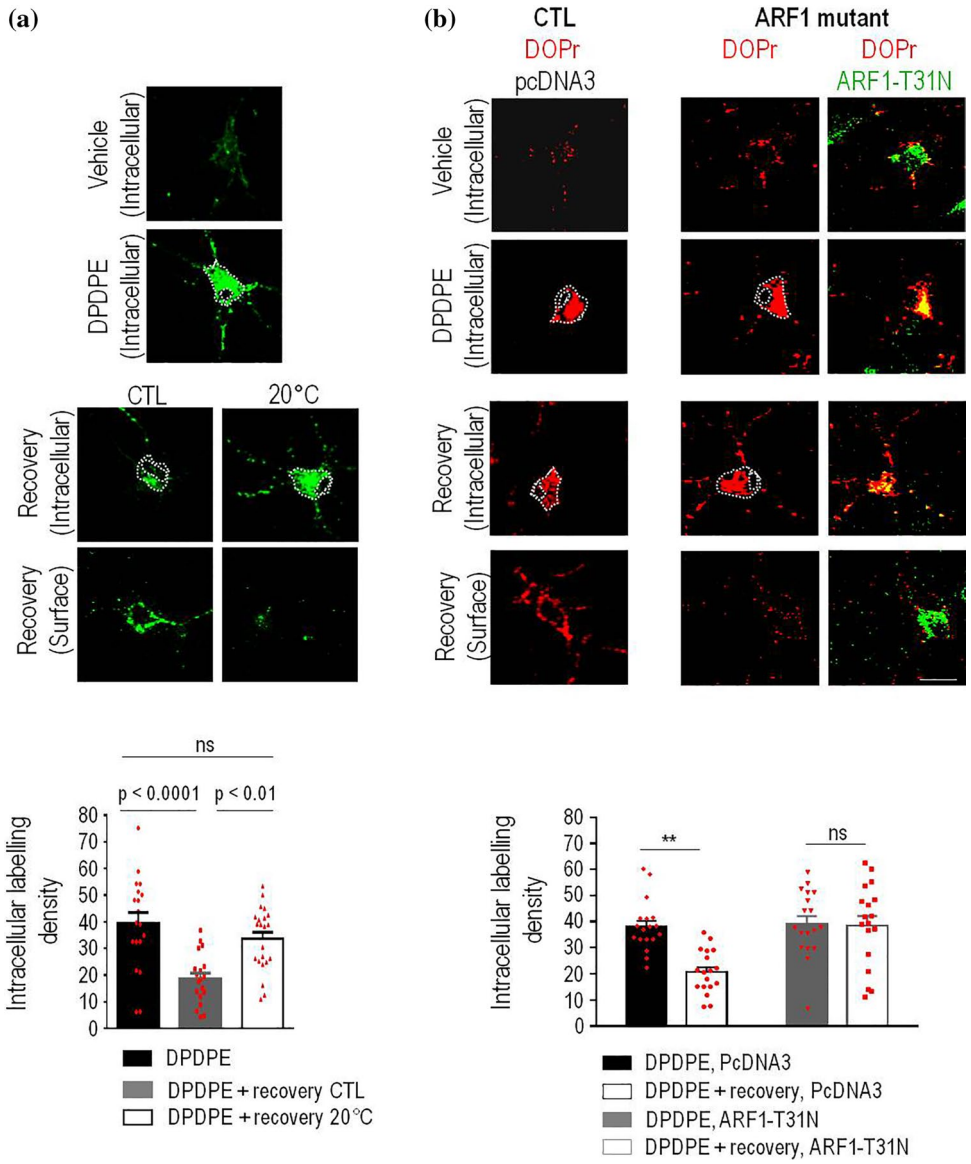

Fig. 5 DOPrs recycle to the membrane from the TGN. Cortical neuron cultures transfected with Flag-DOPrs were first labeled and then treated with DPDPE (10 μM, 60 min) as in previous figures. At the end of treatment cells were either immediately processed for intracellular labeling (upper panel) or allowed to recover from treatment (60 min) either at 37 or 20 °C before revealing intracellular or surface labeling as indicated in lower panels. Scatter plots and histograms show intracellular labeling density (mean ± SEM; $n = 18$) obtained immediately after treatment or following recovery (60 min) as indicated. One-way ANOVA, followed by Tukey's comparisons revealed that there was a significant loss of intracellular labeling in cells that recovered from treatment at 37 °C but not in those that recovered at 20 °C as indicated in the figures (**a**). Cortical neurons were transfected with Flag-DOPrs (red) and pcDNA3 or ARF1-T31N (green) and exposed to vehicle or DPDPE as before. Scatter plots and histograms (mean ± SEM; $n = 18$) represent intracellular labeling density in neurons processed immediately after treatment, or neurons that were allowed to recover. Statistical comparisons by two way ANOVA followed by Tukey's post hoc test revealed significant reduction of intracellular labeling following recovery in pcDNA3 (**$p < 0.001$), but not ARF1-T31N-transfected cells

Interestingly, and despite being sensitive to temperature block (Supplementary figures 5a and 5b) as observed in neurons, DOPr recycling in human HEK cells was neither modified by Y-27632 (10 μM; Supplementary figure 5c) or cytochalasin D (10 μM; Supplementary figure 5d). On the other hand, recycling in HEK cells was sensitive to CID755673 (20 μM), a blocker of carrier biogenesis by protein kinase D [35] (Supplementary figure 5e), which was without effect in rat neuron cultures (Supplementary figure 4b). Hence, while the core mechanism which retrieved DOPrs from LEs to the TGN was conserved across cell types, translocation of the receptor from the TGN to the

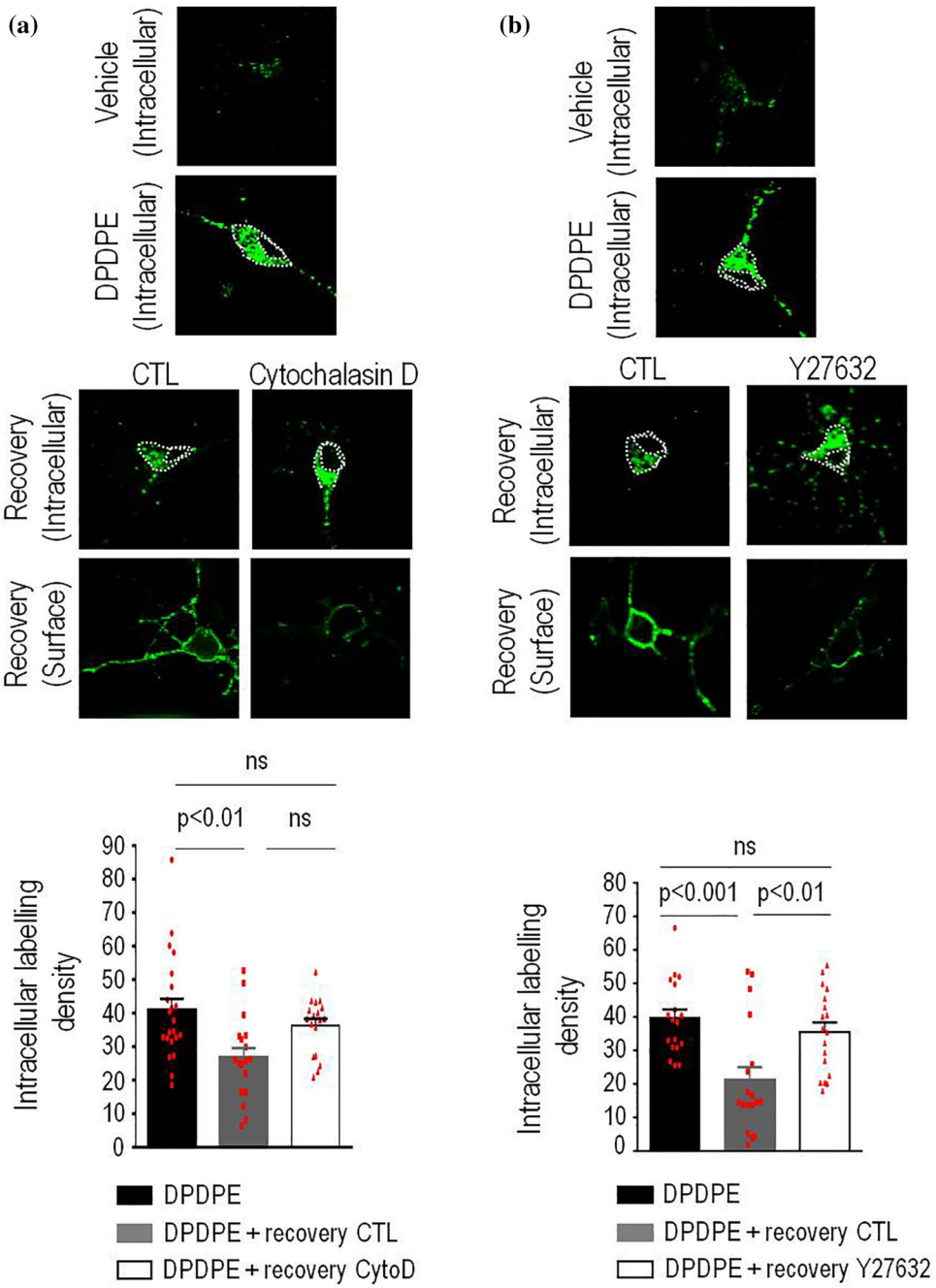

Fig. 6 Actin and ROCK activity are required for DOPr recycling in neurons. Cortical neuron cultures were labeled, treated and processed as in previous figures and allowed to recover from DPDPE treatment in presence or absence of cytochalasin D (10 µM; $n = 18$) (**a**) or Y-27632 (20 µg/20 µl; $n = 18$) (**b**). Scatter plots and histograms (mean ± SEM; $n = 18$) below correspond to intracellular labeling density obtained immediately after treatment or following recovery (60 min) from agonist exposure. Statistical comparisons were completed using one-way ANOVA followed by Tukey's post hoc test which revealed a significant loss of intracellular labeling in cells that recovered from treatment in the absence of inhibitor but not in those that recovered in presence of cytochalasin D (**a**) or Y-27632 (**b**). Statistics shown on the corresponding figures

membrane was cell-type specific, depending on actin and ROCK activity in neurons and PKD in HEK cells.

Finally, because analgesic responses are directly influenced by ligand ability to support DOPr recycling [3, 4], it was of importance to determine whether the described recycling itinerary was relevant to in vivo DPDPE responses. To address this issue, the antiallodynic effect of two equal and consecutive doses of DPDPE (2 × 10 nmol; i.t.) were assessed in rats that were injected either with Y-27632 (20 µg/20 µl; i.t.) or saline prior to the agonist. The increase in threshold for mechanical allodynia that was observed after the first DPDPE injection was similar in rats pretreated with saline or ROCK inhibitor Y-27632 (Fig. 7). In contrast, the second DPDPE injection induced analgesia in rats that had received saline but failed to do so in animals treated with Y-27632.

Discussion

By targeting receptors for degradation or directing them back to the membrane, post-endocytic sorting may considerably influence receptor signaling. For GPCRs this sorting

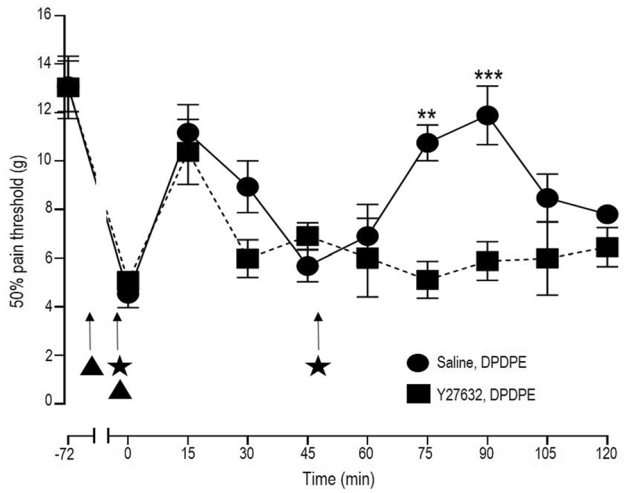

Fig. 7 Rock inhibitor Y-27632 precipitates acute tolerance to DPDPE-mediated analgesia. Mechanical allodynia was induced by intraplantar administration of CFA 72 hs before the experiment. On the day of the experiment rats received an i.t. injection of saline or Y-27632 (20 µg/20 µl) (filled triangles) followed by a second injection of saline or Y-27632 (filled triangles) immediately before DPDPE administration (i.t., 10 nmol) (filled stars). Mechanical thresholds were assessed immediately after DPDPE injection and then every 15 min until return to baseline and, at this time, animals were administered a second identical dose of DPDPE. Results correspond to pressure withdrawal threshold (mean ± SEM) for rats injected with saline + DPDPE ($n = 8$) or with Y-27632 + DPDPE ($n = 7$). Statistical comparisons by two-way ANOVA revealed an effect of time ($p < 0.0001$): an effect of Y-27632 pre-treatment ($p < 0.0001$) and an interaction ($p = 0.0033$). Post-hoc comparisons with Bonferroni correction revealed differences after the second injection of DPDPE in saline and Y-27632-treated groups as indicated in the figure (**$p < 0.01$, ***$p < 0.001$)

step has been traditionally associated with structures originating in early endosomal compartments and, once the decision taken the receptor in question is thought as committed *either* to recycling *or* degradation. Here we report a sorting scheme where DOPrs that are sorted to the degradation path [6–8] can be retrieved from LEs to the TGN, from where they recycle to the membrane completing an itinerary that is necessary for a sustained analgesic response. The core machinery retrieving DOPrs from LE to TGN was conserved in HEK cells and neurons, but TGN-membrane targeting relied upon cell type-specific mechanisms.

Several of our observations indicate that DOPr recycling takes place after sorting for degradation. First, Rab4 and retromer-dependent mechanisms (VPS35) that are classically associated with cargo recovery before sorting to ILVs [20, 23, 26] did not take part in DOPr recycling. Second, observations obtained with an inactive Rab7 mutant additionally pointed to LEs as the site where DOPrs were redirected back to the membrane. Indeed, Rab7 has been proposed as a mechanism of progression from early to late endosomal compartment [22, 39]. Studies using inactive forms of Rab7 (e.g.: Rab7N125I) [26, 40] and more recently siRNA silencing studies [41] have shown that interfering with Rab7 activity traps cargo typically destined to LEs within structures labeled with EE markers. Thus, inhibition DOPr recycling by Rab7N125 is consistent with these observations and indicates that receptors must progress from EEs to LEs before they can regain the membrane. The lack of effect of VPS35 silencing additionally excluded the possibility of DOPrs being sorted for recycling before progressing into MVBs. Finally, DOPr recycling required Rab9 and TIP47, both of which rescue M6PRs to the TGN before LEs fuse with LYS [27, 28]. While Rab9 mediates the actual transport of vesicles from LE to the TGN [42], TIP47 helps stabilize [43] and maintain active Rab9 on the LE membrane [44]. Reciprocally, direct interaction with Rab9 is responsible, at least in part, for TIP47 recruitment to the endosome [44], all of which explain how silencing of either protein may functionally interfere with DOPr recycling from LEs. M6PRs were previously shown to directly interact with TIP47 [27] through sequences that are absent in DOPrs. However, direct DOPr–TIP47 interaction through other residues cannot be excluded.

Together with Rab9/TIP47, DOPr recycling required the ESCRT accessory protein ALIX [29, 30, 45]. Relying on ALIX for recycling is in marked contrast with the role this protein has in sorting PAR1 receptors into ILVs and directing them to degradation [45]. However, in addition to sorting cargo into ILVs, ALIX has other functions [29, 46]. One of such roles is supporting back fusion of ILVs to the endosomal limiting membrane, a mechanism that is used by different pathogens to enter the cytoplasm after traveling concealed within ILVs [47]. It is possible then that similar to these infection agents DOPrs in ILVs rely upon ALIX's back-fusion properties to regain the limiting membrane and become once again available for Rab9/TIP47 retrieval and translocation to the TGN. Figure 8 shows a schematic representation of the proposed recycling path. The mechanism of how a cytoplasmic protein like ALIX, with no access to LE lumen, may promote the fusion of ILVs with the endosomal limiting membrane remains to be fully understood. A possibility that has been previously suggested is that by binding to LBPA and ESCRT-III on the cytoplasmic leaflet ALIX may reorganize the composition of the luminal portion of the endosomal bilayer, increasing the probability of ILV docking [29]. Another, not necessarily exclusive possibility is that ALIX could divert DOPrs away from LEs into a non-degradative compartment from where they can be retrieved by the Rab9/TIP47 complex and recycle back to the membrane. This possibility is reinforced by recent observations indicating that ALIX redirects non-ubiquitinated, stress-stimulated EGFRs away from the canonical degradation path and into melanosome precursors [46]. Ligand-activated EGFRs lacking all lysine residues were similarly

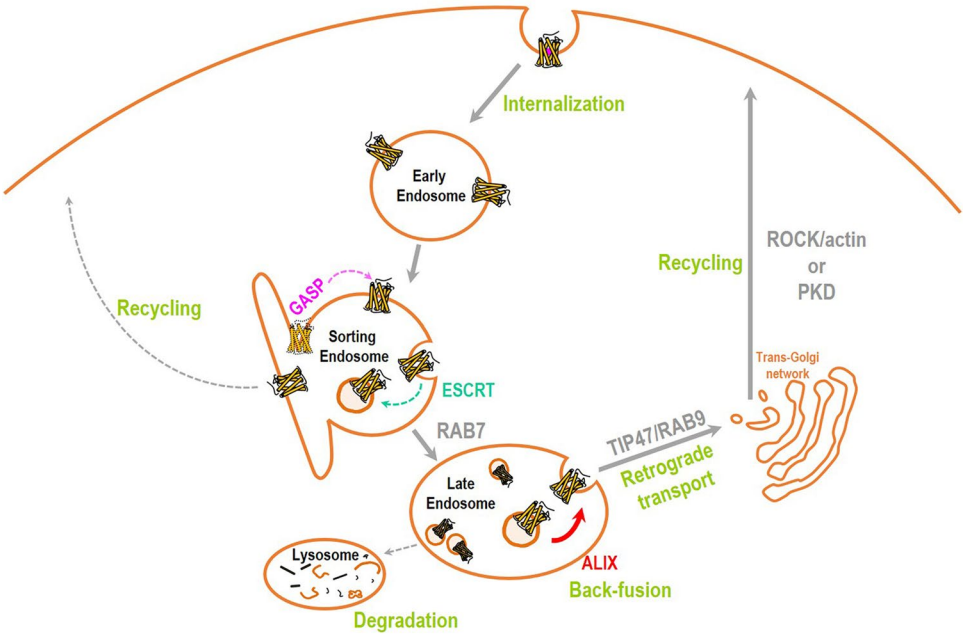

Fig. 8 Schematic representation of proposed recycling itinerary for DOPrs. After internalization GASP-1 excludes DOPrs from the recycling machinery originating at EEs, and the ESCRT complex sorts them into ILVs. By promoting back-fusion of ILVs, ESCRT accessory protein ALIX allows DOPrs to regain the limiting membrane of MVBs/LEs. At the limiting membrane DOPrs become available for translocation by the Rab9/TIP47 retrieval complex which transports them to the TGN. DOPrs then reach the membrane in carriers whose fission from the TGN is cell type-dependent

sorted into these multilaminar structures that do not fuse with LYS, suggesting that absence of ubiquitination could serve as a diversion signal recognized by ALIX [46]. DOPrs resemble stress-activated EGFRs in the sense that they can be sorted into ILVs without ubiquitination [6].

LEs normally function as sorting platforms for M6PRs [48] and for the endopeptidase furin [49], but this compartment had not been previously associated with GPCR recycling to the cell surface. ALIX and the Rab9/TIP47 complex were essential for DOPr recycling both in HEK cells and neurons, indicating a conserved mechanism of LE retrieval for this GPCR. On the other hand, PKD activity was specifically required for DOPr recycling in HEK cells while recycling of neuronal receptors relied upon actin polymerization. Mechanisms of TGN to membrane export are multiple and distinctively engaged depending on cell type and specific membrane domains to which cargo is destined [31]. In neurons ROCK-II, LIMK1 and cofilin locally organize a specialized set of actin filaments which support routing of TGN cargo to the membrane [36, 37]. Our observations that actin polymerization (rather than PKD activity) and ROCK-II activity were required for neuronal DOPrs to recycle to the membrane is consistent with such mechanisms of TGN to membrane transport and in-keeping with a recent report where ROCK-II, LIMK1 and cofilin modulation of the actin cytoskeleton were required for DOPrs to exert sustained Cav2 channel modulation in DRG neurons [50].

In addition to blocking recycling, interfering with ROCK activity precipitated acute analgesic tolerance to DPDPE, pointing to the functional relevance of the described recycling itinerary in maintaining the analgesic response to the agonists. Previous studies showing marked analgesic tolerance for the non-recycling ligand SNC-80 [3, 8], but not for DPDPE, support an inverse relation between DOPr recycling and ligand potential for inducing tolerance [3]. Ligand-specific patterns of recycling have been attributed to differences in ligand susceptibility to endosomal peptidases [4] and to differential stability of DOPr–βarr2 association [3]. In light of the present results it is tempting to speculate that the sustained βarr2 association to DOPrs could prevent organization of a recycling complex between Rab9/TIP47 and the receptor.

In summary, our findings show that retrieval mechanisms which normally rescue non-signaling cargo from imminent lysosomal degradation can also operate on signaling GPCRs. By acting in series with the ESCRT machinery, the Rab9/TIP47 retrieval complex allowed DOPrs that had progressed well into the degradation path to translocate to the TGN, from where they regained the membrane, an itinerary that prevented acute analgesic tolerance.

Methods

DNA constructs, cell culture and transfections

DNA constructs

Murine DOPrs, murine MOPrs and human β2ARs tagged with Flag epitope at the N terminus [7, 51] were kindly provided by Dr. M. von Zastrow (University of California at San Francisco, San Francisco, CA, USA). Rab4-N121I-GFP [20] and Rab7-N125I-GFP [25] were gifts from Dr. T. Hebert (McGill University, Montreal, Quebec, Canada) and ARF1T31N-HA

was provided by Dr. A. Claing (University of Montreal, Montreal, Quebec, Canada) [52].

Primary neuronal cultures

Primary neuronal cultures were prepared from rat postnatal prefrontal cortex (P0-P2) as previously described [3]. Briefly, pups were cryoanaesthetized, brains removed and transferred into ice-cold dissociation solution ($NaS0_4$ 90 mM; K_2SO_4 30 mM; $MgCl_2$ 5.8 mM; $CaCl_2$ 0.25 mM; HEPES 10 mM; glucose 20 mM; pH 7.4). Prefrontal cortex was dissected, digested in papain solution (20 U/ml; 40 min at 37 °C and the product passed through Pasteur pipettes of progressively decreasing diameter for mechanical dissociation. The suspension obtained was centrifuged, cells were then resuspended and diluted to a density of 2.5 million/ml, before being plated on glass coverslips pre-coated with collagen/poly L-lysine (each at 0.1 mg/ml). Culture proceeded in supplemented Neurocell medium (B27 4%; 100 U/ml penicillin–streptomycin; Glutamax 2%; FBS 10%) for 24 h. Coverslips were then transferred to a six-well plate containing 2 ml of Neurocell medium/well and transfected with indicated receptor, dominant negative Rab or ARF1 DNA constructs, using a calcium phosphate transfection protocol as previously described [3]. For siRNA experiments, neurons were transfected with ON-TARGETplus, SMARTpool siRNA (100 pmol/well, Dharmacon) as indicated by manufacturer, 24 h after DNA transfection, using Dharmafect (Dharmacon) as transfection agent. Experiments were carried out 72 h post siRNA transfection and knockdown was verified by Western-blot analysis as described in Nagi et al. [53].

Immortalized cell lines

HEK293 cells (ATCC) were grown in Dulbecco's modified Eagle's medium supplemented with 10% fetal bovine serum and 2 mM L-glutamine (Multicell). Clones stably expressing Flag-DOPr, Flag-MOPr and Flag- β2ARs were generated using G418 at 500 µg/ml as selection agent, as previously described (Invitrogen) [54]. ON-TARGETplus SMARTpool siRNA was transfected onto stable cell-lines at 30–80% confluence in 6- (100 pmol) or 24 (25 pmol) well plates using Dharmafect, 24 h post plating and 72 h before experimentation. For transient expression of recombinant protein, transfections were done 48 h before the experiment using polyethylenimine (Polysciences) according to a previously published protocol [55].

Immunofluorescence

Labeling and quantification of DOPr trafficking in neurons

Immunolabeling of surface receptors for quantification of trafficking was done as previously described [3]. Briefly, Flag-DOPrs, Flag-MOPrs or Flag-β2ARs cultures were incubated at 37 °C with Neurocell medium containing Ca^{2+}-dependent mouse anti-Flag M1 antibody (1:100; Sigma). After 30 min incubation with the antibody, vehicle (0.05% DMSO in Neurocell) or agonist [DPDPE, DAMGO (10 µM), or isoproterenol (1 µM)] were added to the medium for 60 min at the end of which cultured neurons were washed once in calcium-free PBS and then in PBS, all at 37 °C. Half of the cultures were immediately fixed with 4% PFA, permeabilized with PBS/0.1% Triton (20 min at RT), blocked with PBS/BSA 1% (10 min at RT) and incubated with secondary antimouse Alexa 488-conjugated donkey antibody (1:1000; Invitrogen, A21202). The other half of cultured neurons were allowed to recover for 60 min in the absence of ligand before a second round of calcium-free PBS wash was completed before fixation, permeabilization and incubation with secondary antibody. This procedure ensured removal of the antibody bound to Flag-DOPrs still present at the surface, and the exclusive labeling of receptors that were retained intracellularly after internalization or recovery [56]. Another set of neurons was similarly treated with agonist or vehicle and then allowed to recover for 60 min. At this time, they were fixed and incubated with secondary without permeabilization, so as to exclusively reveal Flag-DOPrs that reappeared at the surface during recovery from internalization. Recycling was thus established by taking two independent measures: (1) cytoplasmic labeling density (CLD) lost during recovery from treatment and (2) difference in surface labeling density (SLD) between neurons that were allowed to recover from constitutive (vehicle) or agonist-induced internalization. A schematic representation of the experimental design is provided in Fig. 1a.

Cytoplasmic and surface labeling densities were quantified with ImageJ using a previously described method [57], with small modifications [3]. Thus, total CLD was obtained by measuring fluorescence intensity within the region confined between the external and nuclear perimeters (Supplementary figure 6a), and dividing this value by the corresponding area. Total SLD was defined by calculating the ratio of fluorescence measured within internal and external perimeters of surface-labeled neurons (Supplementary figure 6b), and the corresponding area. Nuclear labeling density (fluorescence within nuclear perimeter/nuclear area) was considered background, and subtracted from total density values just described. Contours defining each of the regions of interest were first drawn on brightened images, and once the trace completed brightness was reset to acquisition conditions, so as to quantify fluorescence intensity. Images were acquired with a FluoView 1000 confocal laser-scanning microscope (Olympus) using a 60× objective. Gain was set for each independent experiment, using calibration slides. These consisted of vehicle- or DPDPE-treated cultures processed for intracellular labeling. Calibration was done by

adjusting gain so as to minimize saturation in the internalization slide while still being able to visualize intracellular labeling in the vehicle slide. Once the parameters were set they were kept constant across all conditions in the same experiment, to ensure that differences in labeling density represented differences in receptor density.

For experiments in which neurons were treated with cytochalasin D (10 μM) or Y-27632 (10 μM) (Selleckchem, product number # S1049), treatment drugs were introduced immediately after agonist washout and remained present in the incubation medium throughout recovery. CID755673 (20 μM) was introduced 24 h before the day of experiment and remained present throughout internalization and recovery process. In neurons where Flag-DOPrs were co-expressed with dominant negative mutants, the receptor was revealed using antimouse Alexa 594-conjugated goat antibody (1:1000; RT; 60 min, Invitrogen, A11005). Rab4-N121I-GFP and Rab7-N125I GFP-tagged mutants were directly visualized while ARF1-T31N-HA was labeled with rabbit anti-HA primary antibody (1:500, Santa Cruz, sc-805) and antirabbit Alexa 488-conjugated goat antibody (Invitrogen, A11034).

DOPr co-localization with compartment markers in neurons

Flag-DOPrs were labeled with anti-Flag M1 antibody (1:500; Sigma) and then processed as above, in order to reveal receptors internalized in vehicle or DPDPE-treated cultures (10 μM, 60 min), which were allowed to recover (60 min) or not from vehicle or agonist exposure. Neurons were then fixed, permeabilized, and blocked with PBS/BSA 1% before incubation for 60 min at RT with antibody for TGN46 (rabbit, 1:1000, Millipore). Cultures were then washed three times in PBS and secondary, Alexa-conjugated antibodies (1:1000) were added to reveal TGN46 and Flag-DOPrs. Colocalization images were acquired using an SP8 HyVolution point scanning confocal microscope at 60× magnification.

DOPr co-localization in HEK cells

Membrane Flag-tagged DOPrs were labeled with first antibody as above, followed by introduction of vehicle or DPDPE (1 μM; 37 °C) for 30 min. Treatment was stopped by ice-cold washes with normal or calcium-free PBS to exclusively label either membrane DOPrs or receptors that had been internalized. Cells were then fixed with 3% PFA (15 min, RT), permeabilized with 0.1% Triton X-100 (15 min) and blocked in PBS/BSA1%. Corresponding fluorescence-conjugated secondary antibody Alexa 594 (1:1000; RT; 60 min) was added. Rab4-N121I and Rab7-N125I GFP-tagged mutants were directly visualized. Images were acquired using a FluoView 1000 confocal laser-scanning microscope (Olympus) using a 60× objective.

Quantification of DOPr trafficking in HEK293 cells

The amount of receptors recycling to the surface was assessed using a previously published ELISA-based method [3]. HEK293 cells expressing Flag-DOPrs, Flag-MOPrs or Flag-β2ARs were grown on 24-well polylysine-coated plates. One hour before inducing internalization with a single dose of DPDPE, DAMGO or isoproterenol (1 μM; 30 min), protein synthesis was blocked with 10 μM cycloheximide that remained present throughout the duration of the assay. At the end of the internalization period, the agonist was removed by washing three times with DMEM at 37 °C. Cells were allowed to recover at either 37 or 20 °C in agonist-free medium (DMEM/HEPES/cycloheximide) for the indicated time periods. In experiments assessing the effects of different blockers on recycling these were introduced upon agonist removal and allowed to remain present throughout recovery. Experiments were stopped by addition of cold PBS, cells fixed for 15 min at 4 °C in PFA (3%), followed by blocking of non-specific binding with PBS/BSA 1%/$CaCl_2$ 1 mM at RT for 30 min. Cells were subsequently incubated with anti-FLAG M1 antibody (1:1000) for 1 h (RT), washed three times and incubated with peroxidase-conjugated (HRP) anti-mouse antibody (1:5000; Amersham Biosciences) for 30 min. After extensive washing, 200 μl of the HRP substrate *o*-phenylenediamine dihydrochloride (*SIGMA FAST™ OPD*, Sigma-Aldrich) was added to each well. The reaction was allowed to proceed for 8 min and stopped using 50 μl of 3 N HCl. 200 μl of the reaction mix was evaluated for optical density (OD) at 492 nM in a microplate reader (Victor3; PerkinElmer). OD readings correspond to the signal generated by receptors at the cell surface. Wells that had more than 30% cell loss during experiment were excluded from the analysis. The total amount of surface receptors internalized by agonist (I_T) was calculated by subtracting OD obtained in the presence of agonist from the OD obtained in the absence of agonist. The amount of internalized receptors that recycled back to the surface were calculated by subtracting the OD value for surface receptors remaining after recycling from the OD remaining after internalization for each condition, and expressed as percentage of I_T.

Animal procedures and behavioral measures

Animals

Adult male Sprague–Dawley (SD) rats, weighing 175–200 g, were purchased from Charles River laboratories (St Constant, QC, Canada) and housed in a controlled environment

on a 12-h dark/light cycle with a free access to food and water. All procedures were approved by the animal care ethic committee of the Université de Sherbrooke (protocol number # 234-14) and conducted according to policies and directives of the Canadian Council on Animal Care and the International Association for the Study of Pain guidelines for pain research on animals.

Inflammatory pain

Unilateral inflammation was induced by intra-plantar administration of 100 µl emulsified complete Freund's adjuvant (CFA) into the right hind paw of SD rats under brief isoflurane anesthesia. CFA was prepared by emulsion of equivalent volume of oil (Calbiochem, catalog number # 344289) and 0.9% sterile saline solution. The volume injected contained approximately 50 µg of lyophilized bacterial membrane (*Mycobacterium butyricum*). Pre-established exclusion criteria included: (1) abnormal paw edema or inflammation, necrosis, scar formation; (2) absence of CFA-induced mechanical allodynia at baseline; (3) more than 10% loss in body weight and (4) premature death.

Two animals were excluded in this study: one died before testing the other failed to show CFA-induced allodynia. The experimenter was not blinded to treatment or outcome, but was unaware of the cellular results which precluded any expectation about behavioral outcome.

Von Frey filament test

Animals were acclimatized to plexiglas enclosures and the mesh floor 1–3 days prior to behavioral testing. Animals were randomly divided into two groups before the first habituation period. 50% mechanical paw withdrawal thresholds were assessed before and 72 h after CFA administration using Von Frey hair filaments as described in Chaplan et al. [58]. Animals were then injected intrathecally either with the selective ROCK1 inhibitor Y-27632 at a dose of 20 µg/20 µl or sterile saline solution. Two hours later, they were intrathecally injected with 10 nmol DPDPE alone or mixed with Y-27632 (20 µg) in a 20-µl final volume, following which they were tested with Von Frey hair filaments every 15 min during. Once threshold levels returned to pre-treatment values, rats received a second *i.t.* administration of DPDPE at the same dose as the first injection to evaluate tolerance development.

Statistical analyses

Neurons

Analyses were done in 'R' [59]. Comparisons in surface labeling between neurons that were allowed to recover from agonist treatment vs neurons recovered from exposure to vehicle (0.05% DMSO) were done by two-tailed, non-paired Student's *t* test ('R code': t.test(data values~treatment, data = u[u$gene==g,], paired=F, alternative="two.sided). Differences in intracellular labeling were analyzed by ANOVA, using Tukey's for post hoc comparisons. One-way ANOVA was used when the effect of different treatments introduced during recovery was assessed ('R code': *v<-aov(formula* = data values *~treatment, data = u[u$gene==g,])*; *tk<-TukeyHSD(v)*). When the effect of silencing different trafficking proteins was determined, two-way ANOVA was used. *('R code': v<-aov(formula=data values~treatment * siRNA silencing effect, data=u[u$gene==g,])*; *tuk<-TukeyHSD(v)*).

HEK cells

For kinetic curves, data were fit by nonlinear regression, and parameters describing curves for different conditions were compared with 'extra sum of squares F test' using Graphpad 6. For comparisons of single time points (e.g.: β2AR recycling ± siRNA VPS35) or for two time points (e.g.: DOPr recycling ± siRNA TIP47; DOPr recycling ± siRNA Rab9) two-tailed, non-paired Student's *t* test or ANOVA two-way were, respectively, used.

Acknowledgements This research was supported by the Natural Sciences and Engineering Research Council of Canada [Grants RGPIN-2015-05213 (to L.G.) and 311997 (to G.P.)] and the Canadian Institutes of Health Research [Grants MOP 123399 and MOP 136871 (to L.G.); MOP 79432 and MOP 324876 (to G.P.)]. L.G. is the recipient of a Chercheur-boursier Senior and I. C. of a doctoral award from the Fonds de la Recherche du Québec-Santé. The authors thank L. Posa for technical assistance in production of supplementary figure 5c and Dr. P. Dallaire for expert advice on statistical analyses.

Author contributions IC and GP conceived the project and wrote the manuscript. IC performed all of the experiments except those of Fig. 6 (done by KA). LG and KA conceived and analyzed animal studies.

Compliance with ethical standards

Conflict of interest The authors declare no competing financial and no financial interests.

References

1. Gaveriaux-Ruff C, Kieffer BL (2011) Delta opioid receptor analgesia: recent contributions from pharmacology and molecular approaches. Behav Pharmacol 22(5–6):405–414. https://doi.org/10.1097/FBP.0b013e32834a1f2c
2. Gendron L, Cahill CM, von Zastrow M, Schiller PW, Pineyro G (2016) Molecular pharmacology of delta-opioid receptors. Pharmacol Rev 68(3):631–700. https://doi.org/10.1124/pr.114.008979
3. Audet N, Charfi I, Mnie-Filali O, Amraei M, Chabot-Dore AJ, Millecamps M, Stone LS, Pineyro G (2012) Differential

association of receptor-Gbetagamma complexes with beta-arrestin2 determines recycling bias and potential for tolerance of delta opioid receptor agonists. J Neurosci 32(14):4827–4840. https://doi.org/10.1523/JNEUROSCI.3734-11.2012
4. Gupta A, Fujita W, Gomes I, Bobeck E, Devi LA (2015) Endothelin-converting enzyme 2 differentially regulates opioid receptor activity. Br J Pharmacol 172(2):704–719. https://doi.org/10.1111/bph.12833
5. Pradhan AA, Walwyn W, Nozaki C, Filliol D, Erbs E, Matifas A, Evans C, Kieffer BL (2010) Ligand-directed trafficking of the delta-opioid receptor in vivo: two paths toward analgesic tolerance. J Neurosci 30(49):16459–16468. https://doi.org/10.1523/JNEUROSCI.3748-10.2010
6. Henry AG, White IJ, Marsh M, von Zastrow M, Hislop JN (2011) The role of ubiquitination in lysosomal trafficking of delta-opioid receptors. Traffic 12(2):170–184. https://doi.org/10.1111/j.1600-0854.2010.01145.x
7. Whistler JL, Enquist J, Marley A, Fong J, Gladher F, Tsuruda P, Murray SR, Von Zastrow M (2002) Modulation of postendocytic sorting of G protein-coupled receptors. Science 297(5581):615–620. https://doi.org/10.1126/science.1073308
8. Pradhan AA, Becker JA, Scherrer G, Tryoen-Toth P, Filliol D, Matifas A, Massotte D, Gaveriaux-Ruff C, Kieffer BL (2009) In vivo delta opioid receptor internalization controls behavioral effects of agonists. PLoS One 4(5):e5425. https://doi.org/10.1371/journal.pone.0005425
9. Trapaidze N, Gomes I, Bansinath M, Devi LA (2000) Recycling and resensitization of delta opioid receptors. DNA Cell Biol 19(4):195–204. https://doi.org/10.1089/104454900314465
10. Archer-Lahlou E, Audet N, Amraei MG, Huard K, Paquin-Gobeil M, Pineyro G (2009) Src promotes delta opioid receptor (DOR) desensitization by interfering with receptor recycling. J Cell Mol Med 13(1):147–163. https://doi.org/10.1111/j.1582-4934.2008.00308.x
11. Henne WM, Buchkovich NJ, Emr SD (2011) The ESCRT pathway. Dev Cell 21(1):77–91. https://doi.org/10.1016/j.devcel.2011.05.015
12. Jacob C, Cottrell GS, Gehringer D, Schmidlin F, Grady EF, Bunnett NW (2005) c-Cbl mediates ubiquitination, degradation, and down-regulation of human protease-activated receptor 2. J Biol Chem 280(16):16076–16087. https://doi.org/10.1074/jbc.M500109200
13. Lauffer BE, Melero C, Temkin P, Lei C, Hong W, Kortemme T, von Zastrow M (2010) SNX27 mediates PDZ-directed sorting from endosomes to the plasma membrane. J Cell Biol 190(4):565–574. https://doi.org/10.1083/jcb.201004060
14. Hislop JN, Marley A, Von Zastrow M (2004) Role of mammalian vacuolar protein-sorting proteins in endocytic trafficking of a non-ubiquitinated G protein-coupled receptor to lysosomes. J Biol Chem 279(21):22522–22531. https://doi.org/10.1074/jbc.M311062200
15. Tanowitz M, Von Zastrow M (2002) Ubiquitination-independent trafficking of G protein-coupled receptors to lysosomes. J Biol Chem 277(52):50219–50222. https://doi.org/10.1074/jbc.C200536200
16. Cho DI, Zheng M, Min C, Kwon KJ, Shin CY, Choi HK, Kim KM (2013) ARF6 and GASP-1 are post-endocytic sorting proteins selectively involved in the intracellular trafficking of dopamine D(2) receptors mediated by GRK and PKC in transfected cells. Br J Pharmacol 168(6):1355–1374. https://doi.org/10.1111/bph.12025
17. Tappe-Theodor A, Agarwal N, Katona I, Rubino T, Martini L, Swiercz J, Mackie K, Monyer H, Parolaro D, Whistler J, Kuner T, Kuner R (2007) A molecular basis of analgesic tolerance to cannabinoids. J Neurosci 27(15):4165–4177. https://doi.org/10.1523/JNEUROSCI.5648-06.2007
18. Rosciglione S, Theriault C, Boily MO, Paquette M, Lavoie C (2014) Galphas regulates the post-endocytic sorting of G protein-coupled receptors. Nat Commun 5:4556. https://doi.org/10.1038/ncomms5556
19. Sonnichsen B, De Renzis S, Nielsen E, Rietdorf J, Zerial M (2000) Distinct membrane domains on endosomes in the recycling pathway visualized by multicolor imaging of Rab4, Rab5, and Rab11. J Cell Biol 149(4):901–914
20. van der Sluijs P, Hull M, Webster P, Male P, Goud B, Mellman I (1992) The small GTP-binding protein rab4 controls an early sorting event on the endocytic pathway. Cell 70(5):729–740
21. Raiborg C, Bache KG, Gillooly DJ, Madshus IH, Stang E, Stenmark H (2002) Hrs sorts ubiquitinated proteins into clathrin-coated microdomains of early endosomes. Nat Cell Biol 4(5):394–398. https://doi.org/10.1038/ncb791
22. Rink J, Ghigo E, Kalaidzidis Y, Zerial M (2005) Rab conversion as a mechanism of progression from early to late endosomes. Cell 122(5):735–749. https://doi.org/10.1016/j.cell.2005.06.043
23. Rojas R, Kametaka S, Haft CR, Bonifacino JS (2007) Interchangeable but essential functions of SNX1 and SNX2 in the association of retromer with endosomes and the trafficking of mannose 6-phosphate receptors. Mol Cell Biol 27(3):1112–1124. https://doi.org/10.1128/MCB.00156-06
24. Temkin P, Lauffer B, Jager S, Cimermancic P, Krogan NJ, von Zastrow M (2011) SNX27 mediates retromer tubule entry and endosome-to-plasma membrane trafficking of signalling receptors. Nat Cell Biol 13(6):715–721. https://doi.org/10.1038/ncb2252
25. Feng Y, Press B, Wandinger-Ness A (1995) Rab 7: an important regulator of late endocytic membrane traffic. J Cell Biol 131(6 Pt 1):1435–1452
26. Press B, Feng Y, Hoflack B, Wandinger-Ness A (1998) Mutant Rab7 causes the accumulation of cathepsin D and cation-independent mannose 6-phosphate receptor in an early endocytic compartment. J Cell Biol 140(5):1075–1089
27. Diaz E, Pfeffer SR (1998) TIP47: a cargo selection device for mannose 6-phosphate receptor trafficking. Cell 93(3):433–443
28. Lombardi D, Soldati T, Riederer MA, Goda Y, Zerial M, Pfeffer SR (1993) Rab9 functions in transport between late endosomes and the trans Golgi network. EMBO J 12(2):677–682
29. Bissig C, Gruenberg J (2014) ALIX and the multivesicular endosome: ALIX in Wonderland. Trends Cell Biol 24(1):19–25. https://doi.org/10.1016/j.tcb.2013.10.009
30. Matsuo H, Chevallier J, Mayran N, Le Blanc I, Ferguson C, Faure J, Blanc NS, Matile S, Dubochet J, Sadoul R, Parton RG, Vilbois F, Gruenberg J (2004) Role of LBPA and Alix in multivesicular liposome formation and endosome organization. Science 303(5657):531–534. https://doi.org/10.1126/science.1092425
31. De Matteis MA, Luini A (2008) Exiting the Golgi complex. Nat Rev Mol Cell Biol 9(4):273–284. https://doi.org/10.1038/nrm2378
32. Ladinsky MS, Wu CC, McIntosh S, McIntosh JR, Howell KE (2002) Structure of the Golgi and distribution of reporter molecules at 20 degrees C reveals the complexity of the exit compartments. Mol Biol Cell 13(8):2810–2825. https://doi.org/10.1091/mbc.01-12-0593
33. Tanowitz M, von Zastrow M (2003) A novel endocytic recycling signal that distinguishes the membrane trafficking of naturally occurring opioid receptors. J Biol Chem 278(46):45978–45986. https://doi.org/10.1074/jbc.M304504200
34. Cao H, Weller S, Orth JD, Chen J, Huang B, Chen JL, Stamnes M, McNiven MA (2005) Actin and Arf1-dependent recruitment of a cortactin–dynamin complex to the Golgi regulates post-Golgi transport. Nat Cell Biol 7(5):483–492. https://doi.org/10.1038/ncb1246
35. Wakana Y, van Galen J, Meissner F, Scarpa M, Polishchuk RS, Mann M, Malhotra V (2012) A new class of carriers that transport

selective cargo from the trans Golgi network to the cell surface. EMBO J 31(20):3976–3990. https://doi.org/10.1038/emboj.2012.235
36. Salvarezza SB, Deborde S, Schreiner R, Campagne F, Kessels MM, Qualmann B, Caceres A, Kreitzer G, Rodriguez-Boulan E (2009) LIM kinase 1 and cofilin regulate actin filament population required for dynamin-dependent apical carrier fission from the trans-Golgi network. Mol Biol Cell 20(1):438–451. https://doi.org/10.1091/mbc.E08-08-0891
37. Camera P, da Silva JS, Griffiths G, Giuffrida MG, Ferrara L, Schubert V, Imarisio S, Silengo L, Dotti CG, Di Cunto F (2003) Citron-N is a neuronal Rho-associated protein involved in Golgi organization through actin cytoskeleton regulation. Nat Cell Biol 5(12):1071–1078. https://doi.org/10.1038/ncb1064
38. Itoh K, Yoshioka K, Akedo H, Uehata M, Ishizaki T, Narumiya S (1999) An essential part for Rho-associated kinase in the transcellular invasion of tumor cells. Nat Med 5(2):221–225. https://doi.org/10.1038/5587
39. Poteryaev D, Datta S, Ackema K, Zerial M, Spang A (2010) Identification of the switch in early-to-late endosome transition. Cell 141(3):497–508. https://doi.org/10.1016/j.cell.2010.03.011
40. Vitelli R, Santillo M, Lattero D, Chiariello M, Bifulco M, Bruni CB, Bucci C (1997) Role of the small GTPase Rab7 in the late endocytic pathway. J Biol Chem 272(7):4391–4397
41. Girard E, Chmiest D, Fournier N, Johannes L, Paul JL, Vedie B, Lamaze C (2014) Rab7 is functionally required for selective cargo sorting at the early endosome. Traffic 15(3):309–326. https://doi.org/10.1111/tra.12143
42. Kucera A, Bakke O, Progida C (2016) The multiple roles of Rab9 in the endolysosomal system. Commun Integr Biol 9(4):e1204498. https://doi.org/10.1080/19420889.2016.1204498
43. Ganley IG, Carroll K, Bittova L, Pfeffer S (2004) Rab9 GTPase regulates late endosome size and requires effector interaction for its stability. Mol Biol Cell 15(12):5420–5430. https://doi.org/10.1091/mbc.E04-08-0747
44. Aivazian D, Serrano RL, Pfeffer S (2006) TIP47 is a key effector for Rab9 localization. J Cell Biol 173(6):917–926. https://doi.org/10.1083/jcb.200510010
45. Dores MR, Chen B, Lin H, Soh UJ, Paing MM, Montagne WA, Meerloo T, Trejo J (2012) ALIX binds a YPX(3)L motif of the GPCR PAR1 and mediates ubiquitin-independent ESCRT-III/MVB sorting. J Cell Biol 197(3):407–419. https://doi.org/10.1083/jcb.201110031
46. Tomas A, Vaughan SO, Burgoyne T, Sorkin A, Hartley JA, Hochhauser D, Futter CE (2015) WASH and Tsg101/ALIX-dependent diversion of stress-internalized EGFR from the canonical endocytic pathway. Nat Commun 6:7324. https://doi.org/10.1038/ncomms8324
47. Le Blanc I, Luyet PP, Pons V, Ferguson C, Emans N, Petiot A, Mayran N, Demaurex N, Faure J, Sadoul R, Parton RG, Gruenberg J (2005) Endosome-to-cytosol transport of viral nucleocapsids. Nat Cell Biol 7(7):653–664. https://doi.org/10.1038/ncb1269
48. Pfeffer SR (2009) Multiple routes of protein transport from endosomes to the trans Golgi network. FEBS Lett 583(23):3811–3816. https://doi.org/10.1016/j.febslet.2009.10.075
49. Chia PZ, Gasnereau I, Lieu ZZ, Gleeson PA (2011) Rab9-dependent retrograde transport and endosomal sorting of the endopeptidase furin. J Cell Sci 124(Pt 14):2401–2413. https://doi.org/10.1242/jcs.083782
50. Mittal N, Roberts K, Pal K, Bentolila LA, Fultz E, Minasyan A, Cahill C, Pradhan A, Conner D, DeFea K, Evans C, Walwyn W (2013) Select G-protein-coupled receptors modulate agonist-induced signaling via a ROCK, LIMK, and beta-arrestin 1 pathway. Cell Rep 5(4):1010–1021. https://doi.org/10.1016/j.celrep.2013.10.015
51. Cao TT, Mays RW, von Zastrow M (1998) Regulated endocytosis of G-protein-coupled receptors by a biochemically and functionally distinct subpopulation of clathrin-coated pits. J Biol Chem 273(38):24592–24602
52. Boulay PL, Schlienger S, Lewis-Saravalli S, Vitale N, Ferbeyre G, Claing A (2011) ARF1 controls proliferation of breast cancer cells by regulating the retinoblastoma protein. Oncogene 30(36):3846–3861. https://doi.org/10.1038/onc.2011.100
53. Nagi K, Charfi I, Pineyro G (2015) Kir3 channels undergo arrestin-dependant internalization following delta opioid receptor activation. Cell Mol Life Sci 72(18):3543–3557. https://doi.org/10.1007/s00018-015-1899-x
54. Audet N, Paquin-Gobeil M, Landry-Paquet O, Schiller PW, Pineyro G (2005) Internalization and Src activity regulate the time course of ERK activation by delta opioid receptor ligands. J Biol Chem 280(9):7808–7816. https://doi.org/10.1074/jbc.M411695200
55. Boussif O, Lezoualc'h F, Zanta MA, Mergny MD, Scherman D, Demeneix B, Behr JP (1995) A versatile vector for gene and oligonucleotide transfer into cells in culture and in vivo: polyethylenimine. Proc Natl Acad Sci USA 92(16):7297–7301
56. Vargas GA, Von Zastrow M (2004) Identification of a novel endocytic recycling signal in the D1 dopamine receptor. J Biol Chem 279(36):37461–37469. https://doi.org/10.1074/jbc.M401034200
57. Scherrer G, Tryoen-Toth P, Filliol D, Matifas A, Laustriat D, Cao YQ, Basbaum AI, Dierich A, Vonesh JL, Gaveriaux-Ruff C, Kieffer BL (2006) Knockin mice expressing fluorescent delta-opioid receptors uncover G protein-coupled receptor dynamics in vivo. Proc Natl Acad Sci USA 103(25):9691–9696. https://doi.org/10.1073/pnas.0603359103
58. Chaplan SR, Bach FW, Pogrel JW, Chung JM, Yaksh TL (1994) Quantitative assessment of tactile allodynia in the rat paw. J Neurosci Methods 53(1):55–63
59. Team RC (2017) R: a language and environment for statistical computing. R Foundation for Statistical Computing, Vienna. https://www.R-project.org/